

N91-24267-20

CHARACTERIZATION OF IRIIDIUM COATED RHENIUM USED IN HIGH-TEMPERATURE, RADIATION-COOLED ROCKET THRUSTERS*

R. H. Stulen, D. R. Boehme, W. M. Clift, and K. F. McCarty
 Sandia National Laboratories
 Livermore, CA 94551-0969

14748

P. 2

SB899064

ABSTRACT

Materials used for radiation-cooled rocket thrusters must be capable of surviving under extreme conditions of high-temperatures and oxidizing environments. While combustion efficiency is optimized at high temperatures, many refractory metals are unsuitable for thruster applications due to rapid material loss from the formation of volatile oxides. This process occurs during thruster operation by reaction of the combustion products with the material surface. Aerojet Technical Systems has developed a thruster cone chamber constructed of Re coated with Ir on the inside surface where exposure to the rocket exhaust occurs. Re maintains its structural integrity at high temperature and the Ir coating is applied as an oxidation barrier. Ir also forms volatile oxide species (IrO_2 and IrO_3) but at a considerably slower rate than Re. In order to understand the performance limits of Ir-coated Re thrusters, we are investigating the interdiffusion and oxidation kinetics of Ir/Re. The formation of iridium and rhenium oxides has been monitored in situ by Raman spectroscopy during high temperature exposure to oxygen. For pure Ir, the growth of oxide films as thin as $\sim 200\text{\AA}$ could be easily detected and the formation of IrO_2 was observed at temperatures as low as 600 C. Ir/Re diffusion test specimens were prepared by magnetron sputtering of Ir on Re substrates. Concentration profiles were determined by sputter Auger depth profiles of the heat treated specimens. Significant interdiffusion was observed at temperatures as low as 1000 C. Measurements of the activation energy suggest that below 1350 C, the dominant diffusion path is along defects, most likely grain boundaries, rather than bulk diffusion through the grains. The phases that form during interdiffusion have been examined by x-ray diffraction. Analysis of heated test specimens indicates that the Ir-Re reaction produces a solid solution phase of Ir dissolved in the h.c.p. structure of Re.

INTRODUCTION

High temperature materials play a key role in the development of advanced rocket thrusters. New applications require ever increasing fuel combustion efficiency, in turn pushing operating temperatures higher, up to and exceeding 2000 C. At these temperatures, thrusters can be rapidly eroded as exhaust gases attack the inner surface, forming highly volatile metal oxides. To overcome this problem, Aerojet Corp. has developed a new structure consisting of a rhenium body coated with a thin layer of iridium. Functionally, rhenium provides mechanical and structural stability at high temperature while the iridium coating increases oxidation resistance. Without iridium, the rhenium would be rapidly eroded by the formation of volatiles such as Re_2O_3 . Exposure of Re to the combustion environment can occur either by diffusion through the Ir coating or loss of the Ir coating. Ir forms volatile oxide species (IrO_2 and IrO_3) but at a considerably slower rate than Re. Understanding the materials properties of the thruster, such as oxide formation, Ir-Re interdiffusion, and Ir-Re phase formation is therefore of crucial importance in understanding potential failure mechanisms and in predicting component life. In this paper we describe measurements of these properties using Surface Raman spectroscopy, x-ray diffraction, and sputter-Auger techniques.

Surface Raman spectroscopy has been shown to be an effective probe of surface oxide phases, capable of being used on materials under realistic operating environments. It has been employed here to examine oxide formation during exposure of Ir, Re, and Pt to O_2 at temperatures as high as 1000 C. Pt was examined since it is a good candidate for applications involving high concentrations of oxygen. X-ray diffraction and Auger spectroscopy have been used to characterize specimens before and after exposure to high temperatures. XRD provides information on Ir-Re intermetallic phases, while sputter-Auger gives concentration profiles as a function of depth for both oxide layers and heat treated Ir-Re diffusion couples. By determining the lattice parameters of the Ir-Re diffusion couples as a function of processing condition, XRD analysis provides information on diffusion and equilibrium concentrations.

EXPERIMENT

In situ oxidation measurements have been made on polycrystalline foil specimens of iridium. Details of the Raman system for these are presented below. XRD and Auger were used to characterize diffusion couples made by sputter depositing a thin coating of iridium on rhenium substrates. Prior to analysis these specimens were subjected to heat treatment in a vacuum furnace. Tantalum or hafnium foil was wrapped around each diffusion sample to getter any residual oxygen that might have been present during the annealing cycle. This procedure minimizes any oxygen attack of iridium which would make analysis of the resulting diffusion profiles difficult.

* This work was supported by NASA Lewis Research Center under contract #NAS-3-25646 as part of a joint program with Aerojet Technical Systems.

Approved for public release; distribution is unlimited.

PRECEDING PAGE BLANK NOT FILMED

358 INTENTIONAL

Raman spectra were obtained in a backscattering geometry using 3 - 10 mW of 488-nm laser radiation focused to a spot ~100 μm in diameter. Use of an optimized spectrograph, equipped with a subtractive/dispersive filter stage and a two-dimensional photon-counting detector, allowed high-quality spectra to be obtained in 5 - 10 minutes. Polycrystalline oxides of Ir, Re, and Pt were obtained from commercial vendors in order to obtain reference Raman spectra. These standard materials were examined in air by both Raman spectroscopy and x-ray diffraction immediately after opening the sealed shipping vials. Raman spectra were collected during the oxidation of Ir foils by heating the metal in a Leitz microscope hot stage. While sealed to the atmosphere, high-purity dry oxygen was flowed through the hot stage.

Auger electron spectroscopy (AES) was done with a Physical Electronics 600 Scanning Auger system. A typical beam size of $1\mu\text{m}$ at 5 Kv and $1\mu\text{A}$ was used as the excitation source. The electron beam was rastered over a $50\mu\text{m}$ square. The Auger depth profiles were done with a 2 Kv argon ion beam with a sputter rate of $170\text{\AA}/\text{Min}$ for Ir. The sputter rate was determined by sputtering through Ir films with a known thickness. Standard PHI Handbook sensitivity factors were used for atomic concentration calculations.

X-ray diffraction techniques were used to identify the phases produced in the different annealing experiments. A Rigaku, 18kW, rotating-anode, diffraction system equipped with a Cu-targeted anode and a 250-mm wide-angle goniometer operated in digital scan mode was used to collect data from the coated specimens. The diffraction spectra were identified by comparison to standard diffraction patterns in the JCPDS (Joint Committee on Powder Diffraction Standards) database.

RESULTS AND DISCUSSION

Raman spectra were obtained for iridium, rhenium, and platinum during or after high temperature exposure to oxygen. In order to interpret the results it was first necessary to obtain phase-pure samples of the metal oxides to use for generating Raman spectra "standards" of known oxide phases. Powders had to be screened with x-ray diffraction to ensure that they contained primarily a single phase before they were used to generate reference Raman spectra. Figure 1 illustrates Raman spectra taken at room temperature for IrO_2 , PtO_2 , and ReO_3 powder specimens.

Since the Ir coating is the oxidation barrier for the thruster, it was the material most studied with the Raman probe. Figure 2 shows spectra before and during oxygen exposure. The three top spectra were taken during cool-down to room temperature after holding at 1000 C for 15 min in oxygen at atmospheric pressure. Two peaks are observed, at a Raman shift of 560 cm^{-1} and 750 cm^{-1} which shift and broaden as a function of temperature. While we have not investigated this

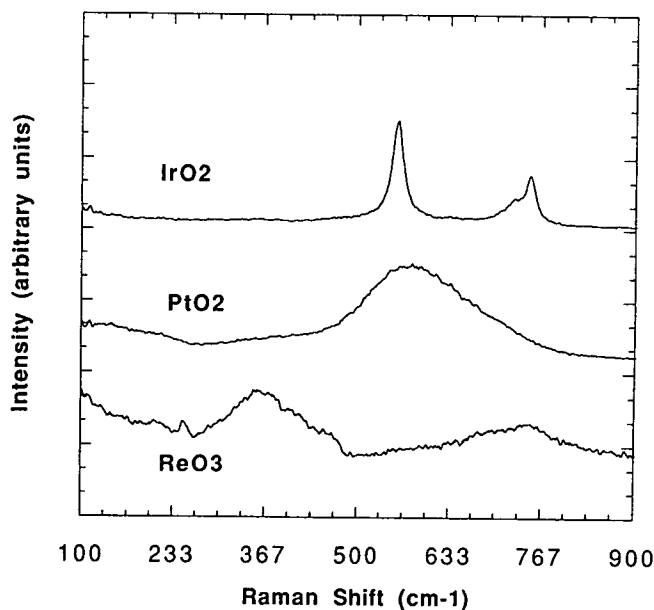


Figure 1. Raman spectra taken at room temperature for IrO_2 , PtO_2 and ReO_3 powder specimens.

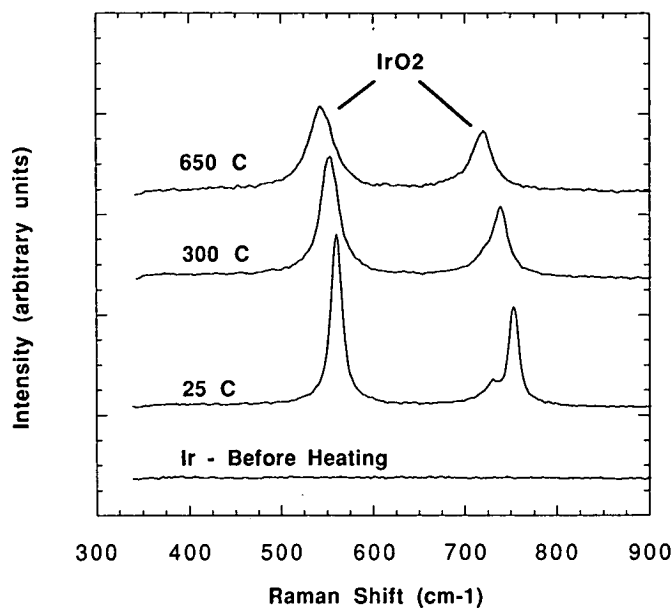


Figure 2. Surface Raman spectra taken on Ir before heating (bottom spectra) and during cool-down (the three top spectra) after holding at 1000°C for 15 min in oxygen at atmospheric pressure.

effect in detail, it is likely due to the loss of oxygen (i.e., formation of IrO_{2-x}) from the material as the temperature is increased.

During the course of these measurements, the window on the high-temperature cell gradually became darker due to the deposition of a thin layer of material. Raman spectra of this window deposit showed it to be identical to both the IrO_2 standard spectra and the 25 C spectra in Fig. 2. These results confirm the notion that oxygen attacks iridium by a process involving the formation and subsequent evaporation of stoichiometric metal oxide (IrO_2).

Additional measurements show that even at temperatures as low as 650 C, a 1-2 hr exposure to oxygen results in a clear Raman signature for IrO_2 . This oxide layer was determined to be approximately 200 Angstroms thick using sputter Auger profiling. It is remarkable that the Raman technique is sensitive to such a thin layer, an indication of the large strength of the scattering cross section in this material.

The oxidation behavior of platinum was also examined with surface Raman spectroscopy. Results on specimens exposed to oxygen at near atmospheric pressure are shown in Fig. 3. The data plotted in the lower curve were taken on a Pt coupon after exposing it at 1250 C for a one hour period. The upper curve is the Raman spectra for the PtO_2 standard. These results are quite striking when compared to the iridium data. The Raman data for Ir exposed under the same conditions (1250 C, 1 hr.) are identical to the 25 C spectra in Fig. 2. Assuming surface oxide formation is a prerequisite to subsequent erosion, Pt appears to be far superior to Ir at these temperatures. Unfortunately, its vapor pressure at higher temperatures prohibits its use (in an unalloyed condition) at 2000 C.

The Ir-Re phase diagram, shown in Fig. 4, contains two solid regions separated by a substantial miscibility gap. We have used X-Ray diffraction (XRD) to examine sintered pellets and thin-film coatings before and after heat treatment to determine the phase composition for comparison to the data in Fig. 4. The pellets, consisting of pressed powders of Ir and Re, weighed approximately 5 g and were 50:50 mixes (atomic %) of pure Ir and Re. After heating the resulting diffraction spectra was identical to spectra observed for heated thin films of Ir on Re foils. Figure 5 compares XRD spectra for a pressed pellet and a thin-film specimen that were both heated to 1500 C in vacuum. The combination of thin-film and pressed pellet studies indicate that, upon heating, the Ir-Re reaction produces a solid solution phase with a hexagonal close packed (h.c.p.) structure whose lattice parameters are similar to those of pure Re¹. The lattice parameters calculated for the characteristic phase produced in the thin-film and pressed pellet samples corresponds to a atomic composition of approximately Re-40%Ir, based on data reported in the earlier studies of these materials. This

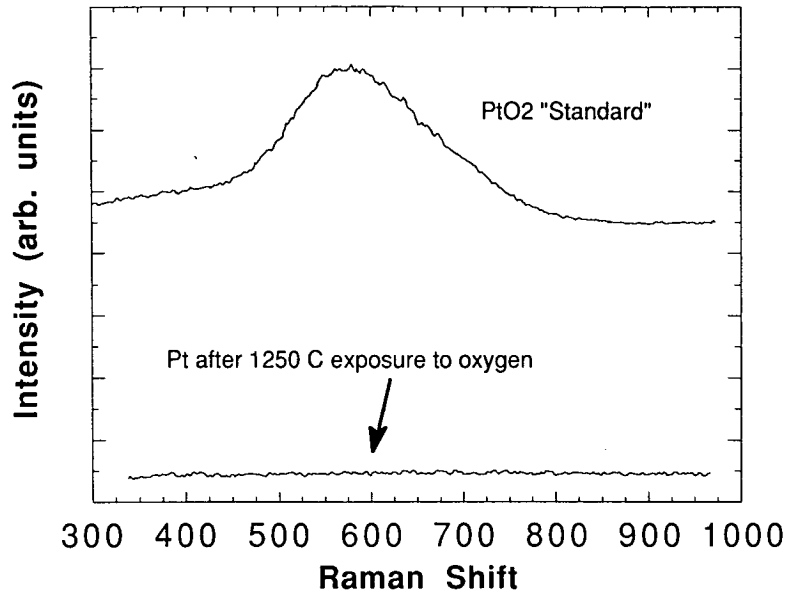


Figure 3. Surface Raman spectra showing the comparison of PtO₂ standard and Pt heated in 1 atm of oxygen. The top spectra for PtO₂ standard and the bottom spectra for Pt foil after heating to 1250°C for 1 h were both taken at room temperature.

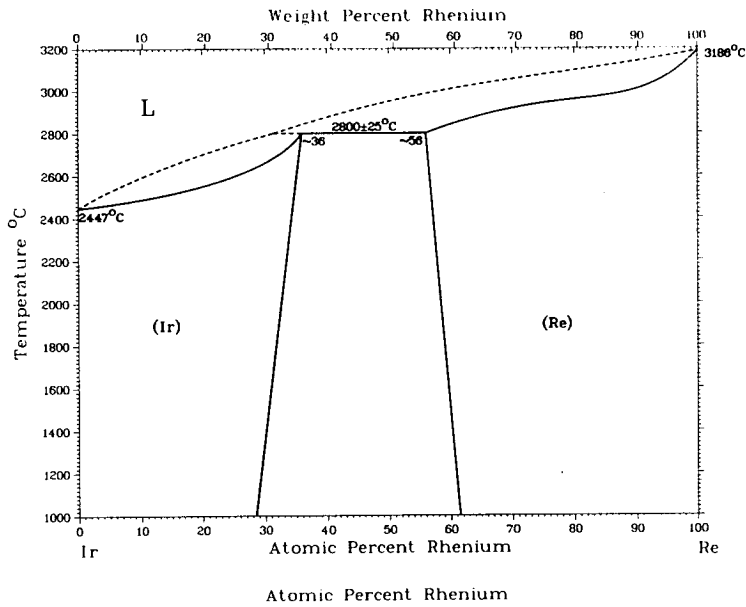


Figure 4. Phase diagram for Ir-Re taken from Shunk, Reference (3).

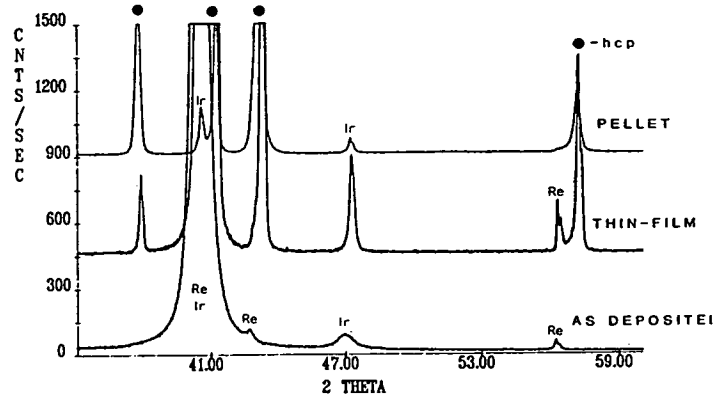


Figure 5. Comparison of X-ray diffraction spectra for heated Ir-Re pellet (top), heated thin-film deposit (middle), and as-deposited thin-film of Ir on Re (bottom). The h.c.p. solid solution phase is identified by the black dots above each of its corresponding peaks. The Re peaks in the heated thin-film (middle spectra) correspond to the underlying Re foil.

composition is just to the right of the miscibility gap shown in Fig. 4 and indicates that the mixing of the two metals at high temperature is dominated by Ir diffusing into Re. If Re were the diffusing species then we would have seen an Ir rich solid solution.

In order to quantify the diffusion constant, we have profiled a number of thin-film samples heated to various temperatures. A rhenium specimen was first coated with approximately 1.5 microns of iridium using a magnetron sputter deposition apparatus and then heated in vacuum. The data in Fig. 6 show the Ir concentration profile, determined by sputter Auger, for a 1200 C / 45 min heat treatment. Only Ir and Re were found to be present in the Auger spectra. The solid line is a fit to the data using an expression for the diffusion of an extended source of limited extent²:

$$C = \frac{1}{2}C_0 \left(\operatorname{erf} \frac{h-x}{2\sqrt{Dt}} + \operatorname{erf} \frac{h+x}{2\sqrt{Dt}} \right).$$

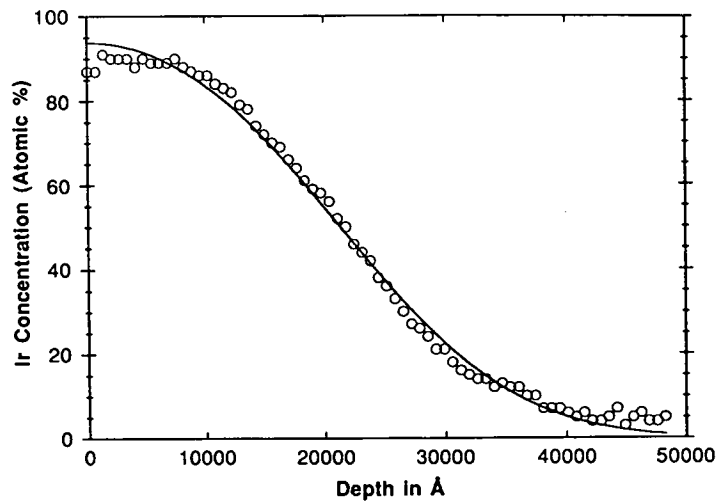


Figure 6. Auger depth profile of Re coated with approximately 1.5 μm of Ir, heated to 1200°C for 45 min. A theoretical fit to the data is shown (solid line). From the fit a diffusivity of $2.4 \times 10^{-12} \text{ cm}^2/\text{sec}$ is calculated for $T=1200^\circ\text{C}$.

Here C is concentration as a function of time and distance, C_0 is the concentration at time equal zero, h is the depth of the Ir coating on Re, t is the time, x is the distance, and D is the diffusion coefficient. From the theoretical fit shown in Fig. 6 we obtain a value for the diffusion coefficient at 1200 C of $D = 2.4 \times 10^{-12}$ cm²/sec. Figure 7 is a plot of the diffusivity obtained in this manner for three different temperatures as a function of $1/T$. A fit to this data gives a value of 1.85 eV for the activation energy associated with diffusion.

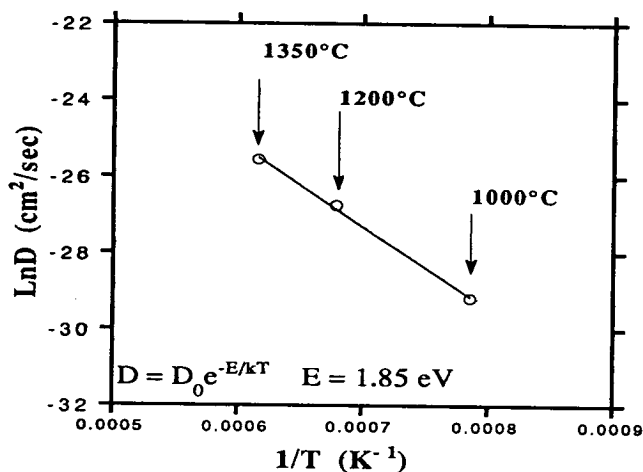


Figure 7. An Arrhenius plot showing the diffusivity of Ir-Re at three different temperatures.

Based on an empirical relationship between melting point and self-diffusion⁴ one would expect the activation energy for bulk diffusion to be approximately 4 eV. Our value of 1.85 eV is significantly less than this value and suggests that, in this case, ideal bulk diffusion is not the rate limiting process. It is known that in addition to normal lattice diffusion, diffusion readily occurs along defects such as grain boundaries and dislocations. For these processes one generally observes activation energies of approximately half that associated with normal lattice diffusion.⁴ Thus we interpret our results in Fig. 7 as evidence for diffusion along grain boundary regions.

Tests done at slightly higher temperatures and much longer times indicate that yet another diffusion mechanism comes into play. Figure 8 shows results for a 1500 C anneal for 14 hours. In this figure we have indicated the predicted profile based on the results discussed above for lower temperature and shorter time. The observed profile is strikingly different. The iridium composition at the surface reaches the same limiting value of between 40 and 50%. Thus under these conditions the diffusion slows down significantly. The same effect was also observed for samples annealed to 1800 C. A number of possibilities exist that might explain this effect. First, since we know there is preferential Ir diffusion into Re it is likely that porosity at the interface between the coating and the substrate develops as a result of grain boundary diffusion. This is the well known Kirkendall effect and would give rise to a decrease in the interfacial area where the diffusion takes place. Secondly, at the higher temperatures it is likely that grain growth occurs. This would decrease the grain boundary surface area and hence decrease the diffusion. Third, the diffusivity may be a strong function of composition so that iridium diffuses much more slowly in Re-Ir 40% than it does under more dilute conditions. At this point we cannot unambiguously distinguish between these various possibilities.

It is interesting to note that we do see evidence for the development of porosity in the films upon heating. Figure 9 shows an annealed film of Ir on Re which before heating was completely smooth. Annealing produced a very porous texture, consistent with the Kirkendall effect and preferential grain boundary diffusion. To determine the cause of the change in the diffusivity will require a more detailed examination of the microstructure before and after heating and further measurements of diffusivity as a function of composition.

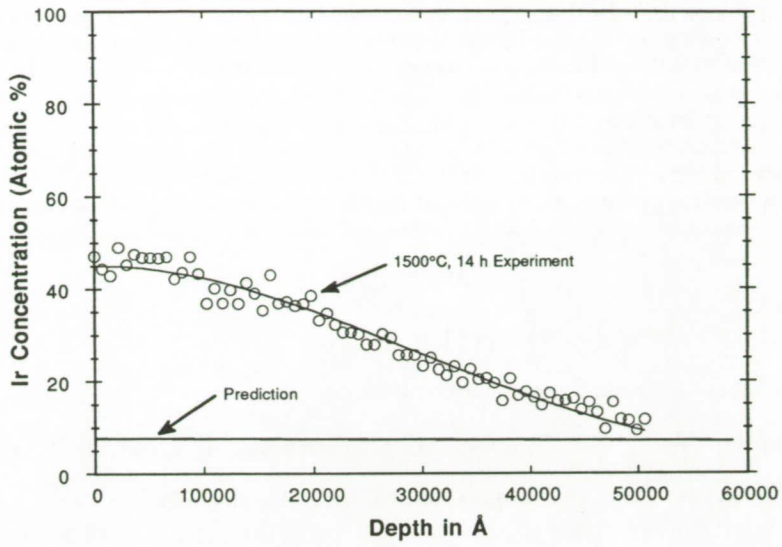


Figure 8. Auger profile of Re coated with approximately 1.5 μ m of Ir, heated to 1500°C for 14h. A theoretical fit to the data is shown (solid line). The bottom line is the predicted profile based on the data from Fig. 7.

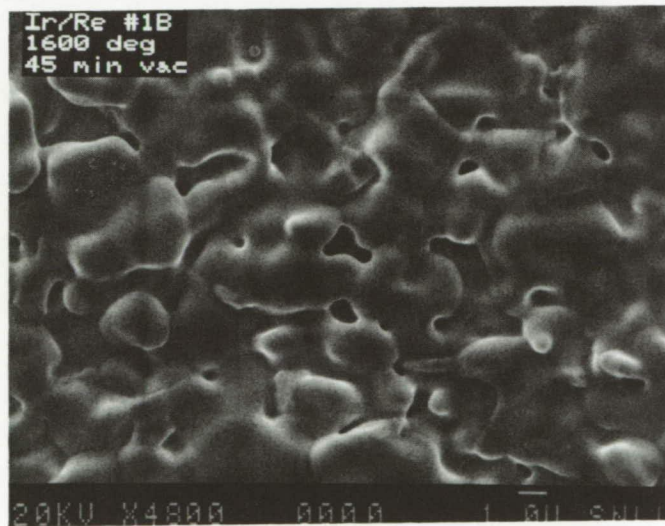


Figure 9. A SEM of an annealed film of Ir on Re which before heating was completely smooth.

ORIGINAL PAGE IS
OF POOR QUALITY

SUMMARY

In conclusion, we have investigated oxidation and interdiffusion for the Ir-Re system using Raman spectroscopy, Auger spectroscopy, and x-ray diffraction. In situ Raman spectroscopy shows that Ir is attacked and etched by oxygen by the formation and desorption of IrO_2 . The Raman cross section is large enough that it is capable of detecting oxide layers as thin as 200\AA . Interdiffusion measurements indicate that for short times and temperatures below 1500 C grain boundary diffusion dominates and that Ir preferentially diffuses into Re. The diffusion profiles are consistent with an activation energy of 1.85 eV . As a result, porosity develops at the interface between the two metals after high temperature annealing. For longer times and temperatures above 1500 C the diffusion appears to slow down significantly. The origin of this effect may be due to interface porosity, microstructural changes, or changes in the diffusion constant as a function of alloy composition.

REFERENCES

1. P. S. Rudman, J. Less Common Metals, 12 (1967) 79-81.
2. "The mathematics of Diffusion," J. Crank, Clarendon Press, 1975, p.15.
3. "Binary Alloy Phase Diagrams, Vol. 2" T. B. Massalski, ed., American Society for Metals, 1986, pg. 1428.
4. "Tracer Diffusion Data for Metals, Alloys, and Simple Oxides, J. Askill, Plenum, p.21